

Leaky-layer seepage: the Verigin function revisited

A. R. Kacimov · Yu. V. Obnosov

Received: 9 November 2006 / Accepted: 19 February 2008 / Published online: 8 March 2008
© Springer Science+Business Media B.V. 2008

Abstract An explicit analytical solution to the problem of steady Darcian seepage into a constant-head subsurface gallery (a straight line segment) placed in a homogeneous rock under a leaky layer of silt deposited in a reservoir is obtained. The third-type boundary condition (linear relation between the head and normal component of the Darcian velocity) along the interface between sediments and rock is tackled by the Verigin function, which satisfies the mixed boundary-value problem conditions in a domain obtained by a conformal mapping of the physical plane (quadrangle) onto an auxiliary plane. This function has three integrable singularities and, unlike Verigin's attempt to construct the second conformal mapping, we use a Signorini-type integral representation. The gallery flow rate is plotted as a function of the gallery size, location under the leaky layer, and the leakage factor, which combines the hydraulic conductivities of the rock and silt, the difference in hydraulic head between the reservoir bottom above the leaky layer and the gallery contour and the silt thickness.

Keywords Analytic functions · Boundary-value problems · Leaky layer · Seepage

1 Introduction

Leaky porous systems are characterised by a layer (AB in Fig. 1) of thickness d made of a low-permeable material (sediment cake) of conductivity k_0 sandwiched between two hydrostratigraphic units (called aquifers in groundwater hydrology and commingled formations in petroleum engineering) or a free-body reservoir and the parent rock (soil) of a much higher thickness and conductivity k_1 . Below we assume that a reservoir with a constant water level h_w is located above a leaky layer, the lower boundary of which coincides with the abscissa axis of a Cartesian system of coordinates Cxy . Along $y < 0$ we have a region of homogeneous rock.

The leaky layer in Fig. 1 can be a clay liner designed for prevention of seepage of hazardous liquids from a reservoir or landfill [1, Sect. 1.2.1, Figs. 1.2–1.3]. As the liner longevity is limited, horizontal backup drains are

A. R. Kacimov (✉)
Department of Soils, Water & Agricultural Engineering, Sultan Qaboos University,
P.O. Box 34, Al-Khod 123, Muscat, Sultanate of Oman
e-mail: anvar@squ.edu.om

Yu. V. Obnosov
Institute of Mathematics and Mechanics, Kazan State University, University Str., 17, Kazan 420008, Russia
e-mail: Yuri.Obnosov@ksu.ru

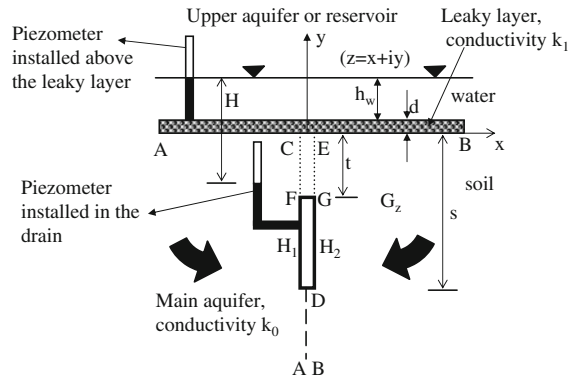


Fig. 1 Vertical cross-section of an aquifer drained by a vertical gallery FDG ; leaky layer $ACEB$ separates the drained aquifer from an upper aquifer (reservoir) with static groundwater (free water body)

installed under the liner. The drains intercept a potential leachate and divert it to special shallow treatment tanks such that contamination of groundwater is prevented. The cake layer in Fig. 1 can build up naturally by deposition of suspended sediments (silt). Geologically, fine sediments sandwiched between two coarser porous massifs are called *leaky layers* (LL) or *aquitards* [2, Sect. 14, Fig. 2.63]. Formation of LL in geotechnical engineering by clogging of reservoir beds causes a major impediment to infiltration from artificial recharge units (e.g. ponds or channels [3]). It has been recently proposed [4] to install horizontal drains under LL and by this means to intensify seepage into the aquifer.

In this paper we study seepage from the reservoir through AB into a gallery FDG placed at a depth of t and having a length of $s - t$. The gallery is a gravel-filled drain whose x -dimension (the size FG in Fig. 1) is negligible compared with $s - t$ (see [5] where the design of galleries is explained). Along FDG , which is modeled mathematically by a cut in the physical plane, the hydraulic head is constant (Fig. 1) because the percolated water fills in the whole gallery. Similar equipotential slot and chimney drains are used in agricultural engineering [6, Chap. 5, Fig. 124] and behind clay cores of earth-, rock-filled dams for phreatic surface control [7, Sect. 5.5–5.6], in permeable foundations beneath concrete dams for reduction of pressure and dam uplift [8] and to remedy contaminated aquifers by air-venting systems for removal of the fluids moved through porous zones targeted by clean-up [9].

Most often LL are modeled by the Dupuit–Forchheimer (DF) approximation, which assumes that the inflow or outflow into the aquifer through LL is accounted by an additional term in the governing equation, which deals with a vertically averaged hydraulic head in the aquifer [10], [6, pp. 398–402], [2, pp. 160–163]. In terms of this simplification, the 2-D Laplace equation becomes an ODE. This “hydraulic” model obliterates the real flow topology, which can be quite puzzling [11]. The DF model is not applicable to the case of Fig. 1 because the gallery drains water from all directions [12].

Verigin [13] pioneered in studying seepage bounded by LL with the framework of a genuinely 2-D model, which seeks a harmonic function in the aquifer ($y < 0$ in Fig. 1) with the third-type condition (TTC) along $y = 0$. TTC, as examined in [12], appears as a limit $d \rightarrow 0$ from the full refraction problem when two harmonic fields (in the aquifer and in the cake, $0 < y < d$) are conjugated. A mathematically equivalent relation between temperature and normal heat flux is also called the Newton or Robin condition in heat-transfer problems where a thin boundary layer between a solid body and ambient cooling or heating fluid is an analogue of the LL in Fig. 1 [14]. The boundary-value problems with TTC were solved in [11, 15, 16] for groundwater applications and in [17, 18] for steady heat transfer.

Verigin [13] suggested a new holomorphic function, which brings some TTC-bordered seepage domains into the realm of conformal mappings. Verigin’s solution for a limiting case of $s \rightarrow t$ when the gallery degenerates into a point sink was later cited in [6, pp. 355–357]. VanDerVeer [19, 20] rediscovered the Verigin function when studying multiple sinks in an aquifer with a step-wise constant head on the top (the so-called polder consisting of a dike maintaining a difference in water levels on its two sides) and a lower boundary consisting of a LL. Anderson [12]

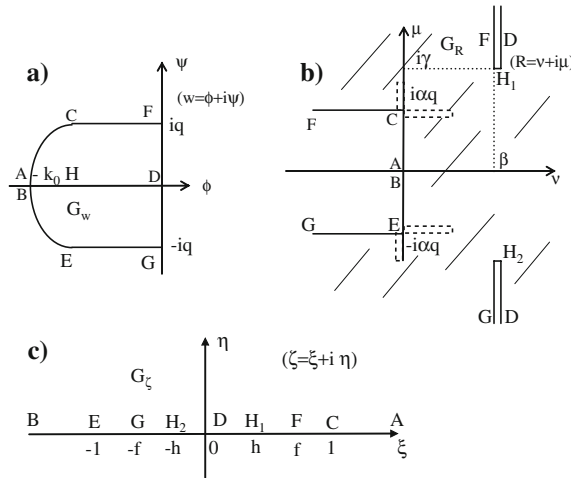


Fig. 2 (a) Complex potential plane, (b) Verigin’s function domain, (c) auxiliary half-plane

warned that the attempts to juxtapose a LL and horizontal no-flow boundaries in [19–21] are not warranted. Indeed, the Verigin function [13] is not able to map straight bedrock boundaries to straight lines in the corresponding domain (or equivalently, in the method of images used in [12] the singularities mirrored about a straight line do not preserve TTC along LL).

Our revision of the Verigin solution [13] to the problem sketched in Fig. 1 is based on a trick that circumvents the conformal mapping of the Verigin function domain [13]. Instead of a cumbersome calculation of conformal-mapping parameters associated with the Schwarz–Christoffel formula we use the most general integral representation [22] of the Signorini-type mixed boundary-value problem, which effectively obviates the very construction of the Verigin domain. This technique is similar to Hamel’s transformation and the integrals that often appear there (see e.g. [23, pp. 303–318]).

New analytical tools, viz. computer-algebra packages [24] and recent theoretical developments in obtaining integral representations to boundary-value problems, which were not available to Verigin, motivate our intention to re-use the old function and to complete the problem attempted by Verigin. Our main objective is to find the seepage rate of the gallery as a function of its size, location and leakage factor.

2 Solution of the boundary-value problem

We introduce the complex physical plane $z = x + iy$. A vertical slit gallery for which the apex and bottom have the ordinates $y = -t$ and $y = -s$, $t < s$, correspondingly, is kept under constant-head conditions and we count this hydraulic head $h(x, y)$ from FDG . We assume that in the reservoir the water level is constant and equals $H > 0$. We assume (as in [13]) that the gallery is the only draining object, so that CF and EG are streamlines. Far from the gallery, water, which saturates completely the half-plane $y < 0$ (seepage domain G_z) in Fig. 1, is static. Owing to seepage, the hydraulic head along $y = 0$ drops from H at A and B to a certain unknown value at C .

Because G_z is symmetric about Cy , we make a vertical cut from point C to D such that the pairs of points (C, E) and (F, G) , although coinciding in G_z (Fig. 1), are different in other characteristic domains shown in Fig. 2.

The Darcian velocity vector $\vec{V} = -k_0 \nabla h$ and complex potential $w(z) = \phi(x, y) + i\psi(x, y)$, $\phi = -k_0 h$ are introduced in a standard manner [6, Chap. 2].

Due to the symmetry of G_z , the velocity vector $\vec{V}(z) = (V_x(x, y), V_y(x, y))$ has to satisfy the symmetry condition $\vec{V}(-\bar{z}) \equiv -\vec{V}(z)$. Correspondingly, the complex potential obeys the identity $\overline{w(-\bar{z})} \equiv w(z)$. The stream function $\psi(x, 0)$ is constant along the streamlines CF and EG and the difference in value is equal to the discharge extracted by the drain $2q$, which is to be found. We assume $\psi = \pm q$ along CF and EG , respectively, i.e., in the

w -plane (Fig. 2a) these two lines (identical in the z -plane) are represented by two different sides of the domain G_w corresponding to G_z . The reference level for ψ is the streamline $DA(B)$, which in Fig. 1 is shown as a dashed ray. We note that the shape of the curve $CABE$ in Fig. 2a is unknown but the potential at point $A(B)$ is $-k_0H$.

The conformal mapping of the quadrangle G_z onto the upper half-plane $\xi > 0$ ($\Im m(\zeta) > 0$) of an auxiliary complex variable $\zeta = \xi + i\eta$ (Fig. 2c) is given by

$$z(\zeta) = -s\sqrt{\zeta^2 - 1}, \tag{1}$$

where the branch of the root $\sqrt{\zeta^2 - 1}$ is fixed to be positive at $\zeta = \xi > 1$. The coordinate f of point F is expressed from (1) at $z(f) = z(-f) = -it$ as

$$f = \sqrt{1 - (t/s)^2}. \tag{2}$$

The leakage condition along $AC(E)B$ reads $V_y(x, 0) = -k_1[H - h(x, 0)]/d$ or

$$\phi'_y(x, 0) = \alpha\phi(x, 0) + \beta \quad \text{at } -\infty < x < \infty,$$

where $\beta = -k_1H/d$ and $\alpha = -k_1/(dk_0)$. Correspondingly, the Verigin function [13] is defined as

$$R(z) = v(x, y) + i\mu(x, y) = \alpha w(z) - iw'(z) + \beta, \tag{3}$$

such that along LL $v(x, 0) = 0$. Clearly, $R(z)$ is holomorphic in G_z , except at the singular points.

The boundary conditions for $w(z)$ and $w'(z) = V_x(x, y) - iV_y(x, y)$ in G_z are

$$\begin{aligned} \phi(0, y) &= 0, & V_y(0, y) &= 0 \text{ along } FDG, \\ \psi(0, y) &= q, & V_x(0, y) &= 0 \text{ along } CF, \\ \psi(0, y) &= -q, & V_x(0, y) &= 0 \text{ along } EG, \\ \frac{\partial\phi(x, 0)}{\partial y} &= \alpha\phi(x, 0) + \beta & & \text{along } AC(E)B. \end{aligned} \tag{4}$$

We emphasize that the boundary conditions along the gallery contour in [25, e.g., p. 247], or well screen (gravel pack) in [11] were set not as in our (4) (i.e., constant head in groundwater problems or constant pressure in petroleum engineering) but as a linear sink of constant intensity. This is a usual “semi-inverse” trick when the flow net generated by the sink (combination of sinks) is obtained from the solution and isopotential (isobaric) lines or surfaces are a posteriori related to a physically real constant head (pressure) contour. In other words, the distributed sink approximation specifies the flow rate of the gallery (well) and determines a constant hydraulic head boundary generating this rate. A detailed analysis revealed that this method has serious limitations when applied to the Muscat [25, pp. 246–250] gallery problem (the details are available from the authors upon request). Our condition along FDG in (4) is direct, physically sound and determines the flow rate as a part of the solution.

In accordance with (4) the Verigin function (3) satisfies the following boundary condition in the ζ -plane

$$\begin{aligned} \Re e(R(\xi)) &= v(\xi) = \beta, & |\xi| &\leq f, \\ \Im m(R(\xi)) &= \mu(\xi) = \alpha q, & f &\leq \xi \leq 1, \\ \Im m(R(\xi)) &= \mu(\xi) = -\alpha q, & -1 &\leq \xi \leq -f, \\ \Re e(R(\xi)) &= v(\xi) = 0, & |\xi| &\geq 1. \end{aligned} \tag{5}$$

The solution of the mixed problem (5) should be searched for in the class of functions finite at points $\zeta = \pm 1$ and infinite (but integrable) at points $\zeta = \pm f$ and $\zeta = 0$.

We introduce, following [22], a new function $r(\zeta)$ such that

$$R(\zeta) = R_0(\zeta)r(\zeta), \tag{6}$$

where

$$R_0(\zeta) = \frac{1}{\zeta} \sqrt{\frac{\zeta^2 - 1}{\zeta^2 - f^2}}. \tag{7}$$

This representation of R as a product of the elementary function (7) and a new unknown function, $r(\zeta)$, transforms the original mixed boundary-value problem (5) to a simpler Schwarz one.

The branch of R_0 is fixed in $\Im m(\zeta) > 0$ by the condition $R_0(\xi) > 0$ ($\arg(R_0(\xi)) = 0$) at $\xi > 1$. For this aim, we select $\arg(\xi) = \arg(\xi \pm 1) = \arg(\xi \pm f) = 0$ at $\xi > 1$. The $\arg(R_0(\xi))$ has the following jumps along the real axes: $\pi/2$ at $\xi = \pm 1$, $-\pi/2$ at $\xi = \pm f$, and $-\pi$ at $\xi = 0$. Accordingly, for $\xi \in \mathbb{R}$ we have: $R_0(\xi) = \text{sign}(\xi) |R_0(\xi)|$ if $|\xi| > 1$ or $|\xi| < f$, $R_0(\xi) = i |R_0(\xi)|$ for $f < |\xi| < 1$, and from (5) and (6) we derive

$$\Re(r(\xi)) = \begin{cases} 0, & |\xi| > 1, \\ \alpha q \text{ sign}(\xi) / |R_0(\xi)|, & f < |\xi| < 1, \\ \beta / R_0(\xi), & |\xi| < f. \end{cases} \tag{8}$$

The function $r(\zeta)$ is integrable at the points $\xi = \pm 1, 0$ and finite at $\xi = \pm f$ and $\xi = \infty$. The solution of the Schwarz problem (8) in this class of functions is expressed through a Cauchy type integral [22]. We note that in [22] an arbitrary mixed boundary-value problem (with an arbitrary index as compared with special cases of the index value, [26, Chap. VI, pp. 472–474] is reduced to a Schwarz integral. Eventually, from (6) the original problem (5) has the following solution

$$R(\zeta) = R_0(\zeta) \left[\frac{\beta}{i\pi} \int_{-f}^f \frac{d\tau}{(\tau - \zeta)R_0(\tau)} + \frac{\alpha q}{i\pi} \int_{(-1,-f) \cup (f,1)} \frac{\text{sign}(\tau) d\tau}{(\tau - \zeta)|R_0(\tau)} + ic_0 \right], \tag{9}$$

where the parameter f is defined in (2) and the constants c_0 and q are to be found. In order to determine these constants we have to evaluate the limit values, $R^+(\xi)$, of the function (9) when $\zeta \rightarrow \xi \in \mathbb{R}$ from the upper half-plane. According to the Plemelj–Sokhotskii formula [26, Chap. I, pp. 37–39] we get:

$$R^+(\xi) = R(\xi) + \beta, \quad |\xi| < f; \quad R^+(\xi) = R(\xi) + i\alpha q, \quad f < |\xi| < 1, \tag{10}$$

where $R(\xi)$ is a principal value of the function (9) at the point $\xi \in \mathbb{R}$. In particular, $R^+(\xi) = R(\xi)$ for $|\xi| > 1$.

Verigin [13] constructed the domain G_R based on (4) as a heptagon (Fig. 2b) where H_1 and H_2 are two points on the gallery, which correspond to two end points of the semi-infinite cuts in Fig. 2b (we note that Verigin’s y -axis was oriented vertically downward).

From the definition (3) of $R(z)$ we can write:

$$\frac{dw}{d\zeta} + i\alpha \frac{dz}{d\zeta} w = i \frac{dz}{d\zeta} [R(\zeta) - \beta] \tag{11}$$

or

$$\frac{dw}{d\zeta} + P_1(\zeta)w = P_2(\zeta), \tag{12}$$

where

$$P_1(\zeta) = i\alpha \frac{dz}{d\zeta}, \quad P_2(\zeta) = i \frac{dz}{d\zeta} (R(\zeta) - \beta)$$

and $dz/d\zeta$ is expressed from (1).

Thus, Eq. 12 is a linear first-order ODE in the complex plane. The solution to the Cauchy problem $w(0) = 0$ for (12) is:

$$w(\zeta) = i e^{-i\alpha z(\zeta)} \int_0^\zeta e^{i\alpha z(\zeta)} z'(\zeta) (R(\zeta) - \beta) d\zeta. \tag{13}$$

Due to the representation (13) and the evident equality

$$\beta \int_0^\zeta e^{i\alpha z(\zeta)} z'(\zeta) d\zeta = -i k_0 H (e^{-i\alpha s \sqrt{\zeta^2 - 1}} - e^{\alpha s}),$$

the condition $w(\infty) = -k_0 H$ (Fig. 2a) is reduced to

$$\int_0^\infty e^{i\alpha z(\zeta)} z'(\zeta) R(\zeta) d\zeta = i k_0 H e^{\alpha s}. \tag{14}$$

The condition $w(f) = iq$ (Fig. 2a) can be converted to

$$\int_0^f e^{i\alpha z(\tau)} z'(\tau) R(\tau) d\tau + qe^{\alpha f} = 0. \tag{15}$$

Equations (14) and (15) constitute a system of linear equations with respect to c_0 and q , which are linked through (9). The simplest form of this system can be deduced using the following properties. The fixed branches of (1), (7) both satisfy the symmetry identities

$$\overline{z(-\bar{\zeta})} \equiv -z(\zeta), \quad \overline{R_0(-\bar{\zeta})} \equiv -R_0(\zeta).$$

and therefore $\overline{z'(-\bar{\zeta})} = z'(\zeta)$. Consequently, for the functions (9), (13) the following identities are true:

$$\overline{R(-\bar{\zeta})} \equiv R(\zeta), \quad \overline{w(-\bar{\zeta})} \equiv w(\zeta).$$

Taking into account (7) we decouple the following singular Cauchy-type integral into a regular (at $\xi \notin (-1, -f)$) integral and an integral which is expressed explicitly by an elementary function:

$$\begin{aligned} \frac{\alpha q}{i\pi} \int_{(-1,-f) \cup (f,1)} \frac{\text{sign}(\tau) d\tau}{(\tau - \zeta) |R_0(\tau)|} &= \frac{\alpha q}{\pi} \int_{(-1,-f) \cup (f,1)} \frac{d\tau}{(\tau - \zeta) R_0(\tau)} \\ &= i\alpha q [1/R_0(\zeta) - \zeta] - \frac{2\alpha q}{\pi} \int_{-1}^{-f} \frac{d\tau}{(\tau - \zeta) R_0(\tau)}. \end{aligned}$$

We use the last integral, the listed symmetry identities, (9) and (10) and write the linear system:

$$a_{11}C_0 + a_{12}Q = b_1, \quad a_{21}C_0 + a_{22}Q = b_2. \tag{16}$$

These expressions involve two dimensionless quantities $Q = q/(k_0H)$ and $C_0 = c_0/k_0$. The dimensionless coefficients in (16) are

$$\begin{aligned} a_{12} &= a \int_1^\infty K(\xi) (R_0^{-1}(\xi) - I_1(\xi)) d\xi - a \int_f^1 K(\xi) I_1(\xi) d\xi, \\ a_{11} &= \int_f^\infty K(\xi) d\xi, \quad a_{21} = \int_0^f K(\xi) d\xi, \quad a_{22} = -a \int_0^f K(\xi) I_1(\xi) d\xi + e^{aS}/S, \\ b_1 &= a \int_f^\infty K(\xi) I_2(\xi) d\xi - e^{aS\sqrt{1-f^2}}/S, \quad b_2 = a \int_0^f K(\xi) I_2(\xi) d\xi, \end{aligned} \tag{17}$$

where

$$K(\xi) = \begin{cases} e^{aS\sqrt{1-\xi^2}}/\sqrt{|\xi^2 - f^2|}, & 0 < \xi < 1, \\ \cos(aS\sqrt{\xi^2 - 1})/\sqrt{\xi^2 - f^2}, & \xi > 1, \end{cases} \tag{18}$$

$$I_1(\xi) = \xi + \frac{2}{\pi} \int_{-1}^{-f} \frac{\tau\sqrt{\tau^2 - f^2} d\tau}{\sqrt{1 - \tau^2}(\tau - \xi)}, \quad I_2(\xi) = \frac{2}{\pi} \int_0^f \frac{\tau^2\sqrt{f^2 - \tau^2} d\tau}{\sqrt{1 - \tau^2}(\tau^2 - \xi^2)}, \tag{19}$$

and

$$T = t/H, \quad a = \alpha H = \frac{\beta}{k_0} = -\frac{k_1 H}{k_0 d}, \quad S = s/H. \tag{20}$$

We shall call a in (20) the leakage factor. All integrals in (17) and (19) exist either in the sense of a principal value or as ordinary improper integrals, i.e., the appropriate isolation of singularities is necessary (see [27] for the details). The integrand of a_{12} has a zero of the second order at infinity according to the representations (18) and (19) and asymptotics:

$$\frac{1}{R_0(\zeta)} = -\zeta + \frac{1 - f^2}{2\zeta} + \frac{3 - 2f^2 + f^4}{8\zeta^3} + O(\zeta^{-5})$$

as $\zeta \rightarrow \infty$ and hence the improper integral in a_{12} of (17) exists.

We used the `NIntegrate` and `CauchyPrincipalValue` routines of *Mathematica* [24, pp.686–689] to carry out the integration.

Upon calculating of c_0 and q , we use (13), (9) and reconstruct the dimensionless complex potential $W(\xi) = w(\xi)/(k_0H) = \Phi(\xi) + i\Psi(\xi)$ at $\zeta = \xi > 1$:

$$W(\xi) = iQ - 1 + e^{i\omega(\xi)} \left\{ H_0 - S \int_1^\xi [K(\tau) - iK_1(\tau)]I(\tau) d\tau \right\}, \tag{21}$$

where

$$I(\xi) = aQI_1(\xi) + aI_2(\xi) - C_0, \quad K_1(\xi) = (\xi^2 - f^2)^{-1/2} \sin \omega(\xi), \tag{22}$$

$$\omega(\xi) = aS\sqrt{\xi^2 - 1}, \quad H_0 = e^{aS\sqrt{1-f^2}} - S \int_f^1 K(\tau)I(\tau) d\tau. \tag{23}$$

Finally, using (19) and (22), we obtain for the real and imaginary parts in (21):

$$\Phi(\xi) = -1 + \cos \omega(\xi)[H_0 - S \int_1^\xi K(\tau)I(\tau)d\tau] - S \sin \omega(\xi) \int_1^\xi K_1(\tau)I(\tau)d\tau, \tag{24}$$

$$\Psi(\xi) = Q + \sin \omega(\xi)[H_0 - S \int_1^\xi K(\tau)I(\tau)d\tau] + S \cos \omega(\xi) \int_1^\xi K_1(\tau)I(\tau)d\tau.$$

A mathematically equivalent problem in heat transfer was solved for an array of semi-infinite galleries ($s - t$ in Fig. 1 infinite but t finite) [28]. In the particular case of one gallery the solution from [28] is reduced to the Verigin limit ($s \rightarrow \infty$). In our notation this limit from [28], written in terms of the velocity potential along AB , reads:

$$\Phi(X) = \frac{2}{\pi} \left[\int_X^\infty \frac{\sin a(X - u)du}{\sqrt{u^2 + T^2}} - \frac{1}{T} \frac{K_0(-aT)}{K_1(-aT)} \int_X^\infty \cos a(u - X) \left(1 - \frac{u}{\sqrt{u^2 + T^2}} \right) du \right] - 1, \tag{25}$$

where $X = x/H$ and K_0 and K_1 are Macdonald functions.

3 Results and discussion

Figure 3a shows the dimensionless inflow half-rate $Q(T)$ calculated from (16) for $a = -5 \times 10^{-2}$ and for the following depths of point D in Fig. 1: $S = 0.1, 0.2, 0.3$ (curves 1–3, correspondingly). Figure 3b shows the same sequence of curves but $a = -5 \times 10^{-3}$. As is obvious from the curves and from the comparison theorems from [29, Sects. 1.1 and 1.2], an increase of H, t , and s increases the flow rate. From Fig. 3a, b we see that Q is most sensitive to the gallery size, $S - T$, for small $S - T$.

Figure 4 shows Q as a function of the leakage factor for $S = 0.2$ and $T = 0.05, 0.1, 0.15$ (curves 1–3, correspondingly). From this figure we see that the effect of the leakage factor a on Q is most pronounced for small $|a|$. This implies that, if maximal infiltration intensity from a reservoir bottom is targeted, even a thin sediment cake (d in (20) defining a) should be scraped.

In Fig. 5 we show $\Phi_C(T)$ (curve 1) calculated from (24) for $S = 1$ and $a = -1$. Curve 2 shows the solution $\Phi_{CS}(T)$ calculated from (25) for the same a . At small depth of the gallery, T , the two curves practically coincide, i.e., our solution fits well the limiting ($S = \infty$) case from (25). This implies, in particular, that our finite-length gallery is almost equivalent (in the sense of head depression) to the semi-infinite gallery from (25). Therefore, the excessive size of the gallery adds little to the seepage rate. As $T \rightarrow 1$, we have $S - T \rightarrow 0$ in our solution and $\Phi_C \rightarrow -1$, i.e., flow vanishes and $Q \rightarrow 0$. We note that H is constant in this limit while the point sink requires $\Phi \rightarrow -\infty$ at the singularity.

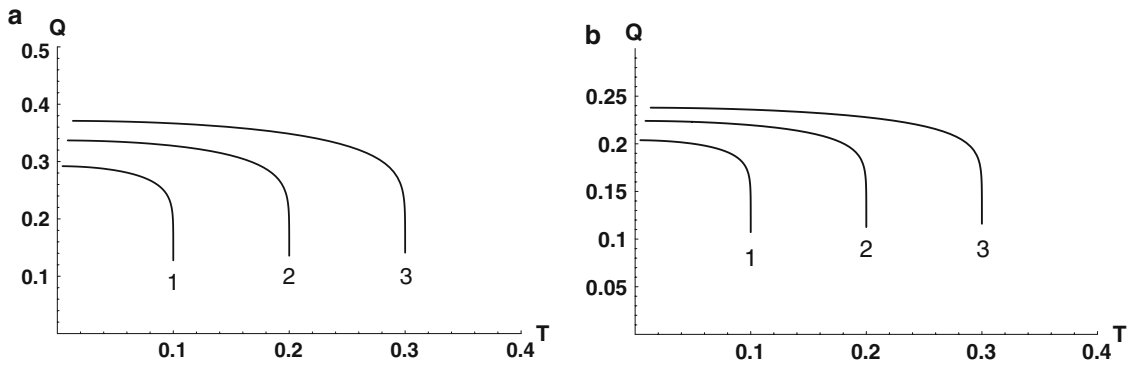


Fig. 3 Seepage flow half-rate Q as a function of T , $S = 0.1, 0.2, 0.3$ (curves 1–3, correspondingly), (a) $a = -5 \times 10^{-2}$, (b) $a = -5 \times 10^{-3}$

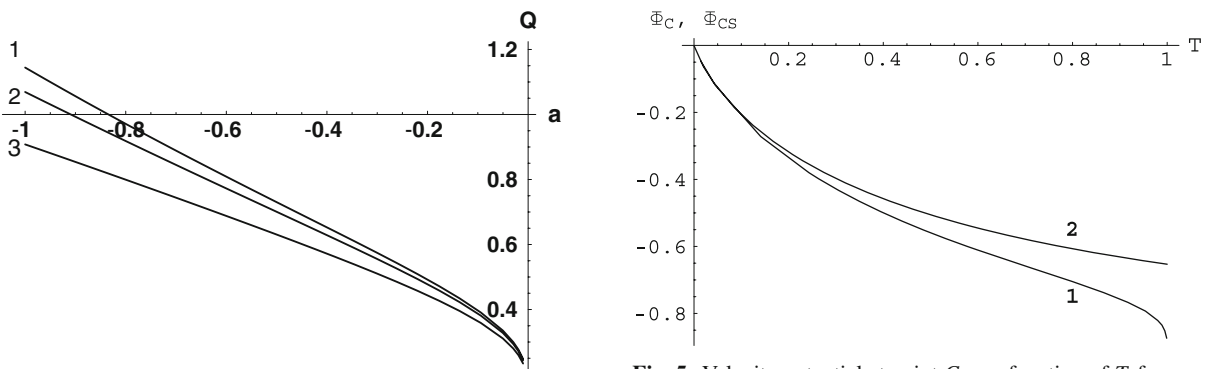


Fig. 4 Half-rate Q as a function of a for $S = 0.2$ and $T = 0.05, 0.1, 0.15$ (curves 1–3, correspondingly)

Fig. 5 Velocity potential at point C as a function of T for $a = -1$, our solution with $S = 1$ (curve 1) and Strakhov’s solution with $S = \infty$ (curve 2)

4 Concluding remarks

The third-type boundary condition is very common in heat-transfer models, where it describes a locally 1-D Fourier-law heat flux to/from a flowing constant-temperature gas or liquid from/to a non-isothermic solid body. Subject to this condition, 2- and 3-D steady (the Laplace equation) and transient (the diffusion equation) problems can be effectively solved analytically in domains (rectangle, cylinder, and sphere) where the variables separate [30, Chaps.5,7,9]. In mathematically equivalent identical seepage problems [2, Sects.14–15], this condition (a local 1-D Darcy law) is relatively rare because it models fluid leakage through a thin low-permeable LL. In physical domains with no separation of variables in PDEs describing heat transfer or seepage, conformal mappings do not work, if the third-type condition is involved, because a characteristic domain (complex potential, hodograph, Zhukovskii function), which can be easily constructed for the Dirichlet (first) or Neuman (second) boundary conditions, is not a standard polygon.

The function discovered in [13] “straightens” the polygon boundary, which corresponds to the LL, and therefore the conformal mapping can, in principle, be constructed. This paper exploits the function from [13] but the technique of obtaining this function is different from the approach suggested in [13]: instead of the Schwarz–Christoffel formula for the mapping we solved a mixed boundary-value problem, i.e., one where the real and imaginary parts of a holomorphic function are specified intermittently on different segments of an auxiliary half-plane.

It is well-known that for polygonal domains in the characteristic (in our case, Verigin) plane one has two options to express a holomorphic function through an auxiliary variable: either the Schwarz–Christoffel formula or an integral representation of the general Hilbert problem [6, pp.206–208]. We advocate the second approach, which was utilised in [27,31,32] for different porous-media flows. The integral representations of holomorphic functions,

which satisfy a mixed problem, are used after Signorini and Keldysh–Sedov [26, Chap. VI, pp. 472–474] in various applications of continuum mechanics, but the most general case of the integral solution has been obtained in [22], where the reconstructed function had arbitrary integrable singularities.

Our final solution, i.e., the complex physical coordinate and the Verigin function, expressed through an auxiliary variable, makes possible—through computation of singular, proper and improper integrals—the analysis of the seepage flow rate as a function of physical parameters of the problem, viz. the drain size, depth, LL thickness, conductivities of the bulk aquifer and the sediments and the difference in the hydraulic head between the drain and reservoir, from which fluid seeps into the drain. All these parameters have equivalents in heat conduction, where the gallery corresponds to a heat-generating device and LL is a cooling surface [28]. Our solution can also be used in estimates of the efficiency of the shut-off of oil wells drilled in complex geological conditions of Oman where thin shale layers adjacent to horizontal wells obstruct water flooding. Therefore, if we turn Fig. 1 upside down, then *CFDGE* can be viewed as a part of a gallery blocked (e.g. by tamponage, cementing, packers, elastomers, etc., see [33] for details) from water flooding. LL impedes upconing and early breakthrough of water from the oil–water contact to a horizontal well beneath *CFDGE*.

Acknowledgements This study was supported by Sultan Qaboos University, project CL/SQU-UAEU/0/3/02 and the Russian Foundation for Basic Research, grant 06-01-81019-Bel_a. Helpful comments by O.Strack, two anonymous referees and discussions with F.Marketz (Petroleum Development Oman - Shell) are appreciated.

References

1. Rowe RK, Quigley RM, Booker JR (1995) Clayey barrier systems for waste disposal facilities. Chapman & Hall, London
2. Strack ODL (1989) Groundwater mechanics. Prentice Hall, Englewood Hills
3. Kacimov AR (2008) Maximisation of water storage in back-filled and lined channels and dimples subject to evaporation and leakage. *J Irrigation Drainage ASCE* 134:101–106
4. Prathapar S, Perret J, Seckler D (2004) A new approach to bypass silt deposition in recharge dams. In: Proceedings of Regional Workshop on Management of Aquifer Recharge and Water Harvesting in Arid and Semi-arid Regions of Asia. Yazd, Iran, pp 69–79
5. Voutchkov N (2005) Well design and construction In: Lehr J (ed) Water encyclopedia. V.4 groundwater. Wiley, Hoboken, New Jersey, pp 87–91
6. Polubarinova-Kochina PYa (1977) Theory of groundwater movement. Nauka, Moscow (in Russian)
7. Cedergren HR (1989) Seepage, drainage, and flow nets. Wiley, New York
8. Romanova EYa (1956) The influence of a crack in the upstream apron on seepage under a dam. In: Mikhailov KA (ed) Problems of calculation of seepage through hydraulic structures, vol 23. GILSA, Moscow (in Russian)
9. Hunt B, Massmann J (2000) Vapor flow to trench in leaky aquifer. *J Environ Eng ASCE* 126:375–381
10. Bakker M (1999) Simulating groundwater flow in multi-aquifer systems with analytical and numerical dupuit-models. *J Hydrol* 222:55–64
11. Bruggeman GA, Veling EJM (2005) Nonmonotonic trajectories to a partially penetrating well in a semiconfined aquifer. *Water Resour Res* 42 WO2501. doi: [20.1029/2005WR003951](https://doi.org/10.1029/2005WR003951)
12. Anderson EI (2000) The method of images for leaky boundaries. *Adv Water Resour* 23:461–474
13. Verigin NN (1949) On calculation of subsurface water uptake in conditions of 2-d groundwater movement. *DAN SSSR* 64:183–186 (In Russian)
14. Kacimov AR, Obnosov YuV (2000) Conduction through a grooved surface and sierpinsky fractals. *Int J Heat Mass Transfer* 43:623–628
15. Anderson EI (2003) An approximation for leaky boundaries in groundwater flow. *J Hydrol* 274:160–175
16. Kacimov AR, Obnosov YuV (2001) Semipermeable boundaries and heterogeneities: modeling by singularities. *J Hydrol Eng ASCE* 6:217–224
17. Malov YuI, Martinson LK, Pavlov KB (1974) Solution of some mixed boundary-value heat conduction problems. *J Eng Phys Thermophys* 27:335–340
18. Minasyan RS (1952) On a mixed boundary-value problem for the laplace equation in a rectangle. *Prikl Mat Mekh* 16:291–304 (in Russian)
19. Van Der Veer P (1978) Exact solutions for two-dimensional groundwater flow problems involving a semi-pervious boundary. *J Hydrol* 37:159–168
20. Van Der Veer P (1994) Exact solutions for two-dimensional groundwater flow in a semiconfined aquifer. *J Hydrol* 156:91–99
21. Bruggeman GA (1999) Analytical solutions of geohydrological problems. Elsevier, Amsterdam

22. Obnosov YuV (1981) Solution of a mixed boundary-value problem in the theory of analytic functions. *Izv VUZ Mat (Soviet Mathematics)* 10:75–79
23. Muscat M (1946) *The flow of homogeneous fluids through porous media*. I.W. Edwards Inc, Ann Arbor
24. Wolfram S (1991) *Mathematica: A system for doing mathematics by computer*. Addison-Wesley
25. Muscat M (1949) *Physical principles of oil production*. McGraw Hill, New York
26. Gakhov FD (1977) *Boundary value problems*, 3rd edn. Nauka, Moscow, (In Russian). Engl. translation of the 2nd edn. (1966) Addison Wesley, New York
27. Youngs EG, Kacimov AR, Obnosov YuV (2004) Water exclusion from tunnel cavities located in the saturated capillary fringe with uniform precipitation flowing to a water bearing substratum. *Adv Water Resour* 27:237–243
28. Strakhov IA (1972) Heat transfer problem for a semi-infinite body heated by thin parallel plates. *J Eng Phys Thermophys* 23: 331–338
29. Goldstejn RV, Entov VM (1994) *Qualitative methods in continuum mechanics*. Wiley, New York
30. Carslaw HS, Jaeger JC (1959) *Conduction of heat in solids*. Oxford University Press, Oxford
31. Kacimov AR, Obnosov YuV (2006) Strip-focused phreatic surface flow driven by evaporation: analytical solution by the Riesen-ampf function. *Adv Water Resour* 29:1565–1571. doi: [10.1016/j.advwatres.2006.01.004](https://doi.org/10.1016/j.advwatres.2006.01.004)
32. Kacimov AR, Obnosov YuV (2008) Analytical solution to 2D problem for an anticline-diverted brine flow with a floating hydrocarbon trap. *Transp Porous Media* 71(1):39–52. doi: [10.1007/s11242-007-9110-y](https://doi.org/10.1007/s11242-007-9110-y)
33. Kacimov AR, Marketz F, Pervez T (2008) Optimal placement of a wellbore seal impeding seepage from a tilted fracture. *Appl Mathemat Model (Elsevier)* (in press)